Mexiletine block of wild-type and inactivation-deficient human skeletal muscle hNav1.4 Na^+ channels

Ging Kuo Wang[1], Corinna Russell[1] and Sho-Ya Wang[2]

[1] *Department of Anaesthesia, Harvard Medical School and Brigham and Women's Hospital, Boston, MA, USA*
[2] *Department of Biology, State University of New York at Albany, Albany, NY, USA*

Mexiletine is a class 1b antiarrhythmic drug used for ventricular arrhythmias but is also found to be effective for paramyotonia congenita, potassium-aggravated myotonia, long QT–3 syndrome, and neuropathic pain. This drug elicits tonic block of Na^+ channels when cells are stimulated infrequently and produces additional use-dependent block during repetitive pulses. We examined the state-dependent block by mexiletine in human skeletal muscle hNav1.4 wild-type and inactivation-deficient mutant Na^+ channels (hNav1.4-L443C/A444W) expressed in HEK293t cells with a β1 subunit. The 50% inhibitory concentrations (IC_{50}) for the inactivated-state block and the resting-state block of wild-type Na^+ channels by mexiletine were measured as 67.8 ± 7.0 μM and 431.2 ± 9.4 μM, respectively ($n = 5$). In contrast, the IC_{50} for the block of open inactivation-deficient mutant channels at +30 mV by mexiletine was 3.3 ± 0.1 μM ($n = 5$), which was within the therapeutic plasma concentration range (2.8–11 μM). Estimated on- and off-rates for the open-state block by mexiletine at +30 mV were 10.4 μM^{-1} s^{-1} and 54.4 s^{-1}, respectively. Use-dependent block by mexiletine was greater in inactivation-deficient mutant channels than in wild-type channels during repetitive pulses. Furthermore, the IC_{50} values for the block of persistent late hNav1.4 currents in chloramine-T-pretreated cells by mexiletine was 7.5 ± 0.8 μM ($n = 5$) at +30 mV. Our results together support the hypothesis that the *in vivo* efficacy of mexiletine is primarily due to the open-channel block of persistent late Na^+ currents, which may arise during various pathological conditions.

(Resubmitted 15 September 2003; accepted after revision 7 November 2003; first published online 7 November 2003)
Corresponding author G. K. Wang: Department of Anaesthesia, Harvard Medical School and Brigham and Women's Hospital, Boston, MA, USA. Email: wang@zeus.bwh.harvard.edu

A variety of rare missense mutations in the α-subunit of the skeletal muscle Nav1.4 Na^+ channel cause heritable muscle diseases such as paramyotonia congenita, hyperkalaemic periodic paralysis, and potassium-aggravated myotonia (Lehmann-Horn & Jurkat-Rott, 1999; Cannon, 2002). Fast inactivation is partially disrupted by most mutations, and some of mutations also cause a shift in activation and/or altered slow inactivation. A partial disruption of fast inactivation often results in persistent late Na^+ currents during prolonged depolarization. Model simulations show that these functional defects are sufficient to cause repetitive discharges in myotonia or to induce paralysis.

The class 1b antiarrhythmic drug mexiletine has been taken orally for ventricular arrhythmias (Roden, 2001). It has also been used to reduce or prevent myotonia (Jackson *et al.* 1994; Lehmann-Horn & Jurkat-Rott, 1999), to treat long QT–3 syndrome (Schwartz *et al.* 1995), and to alleviate neuropathic pain (Chabal *et al.* 1992). Mexiletine is an analogue of the local anaesthetic (LA) lidocaine that, like most LAs, produces both tonic block when cells are stimulated infrequently and additional use-dependent block of Na^+ current during repetitive pulses (Hille, 2001; Catterall & Mackie, 2001). Mexiletine displays different efficacies for different Na^+ channel states. The resting-state affinity ($K_R = 650$ μM) for mexiletine is low, whereas the inactivated-state affinity ($K_I = 28.3$ μM) is ~22 times higher (Takahashi & Cannon, 2001). The therapeutic plasma concentration (2.8–11 μM), however, is much lower than these estimated values.

Mexiletine block of mutant cardiac Na^+ channels that cause long QT syndromes was previously examined by Wang *et al.* (1997), who found that the affinity of the mutant channels in the inactivated state was similar to the wild-type, with a 50% inhibitory concentration (IC_{50}) of 15–20 μM. Interestingly, block of the late-opening channels by mexiletine was achieved at significantly lower

 DOI: 10.1113/jphysiol.2003.054973

concentrations, with an IC_{50} of 2–3 μM at –20 mV. These authors suggested that this selective targeting of the persistent late Na^+ currents by mexiletine is important for its therapeutic intervention in cardiac diseases.

We were interested in whether mexiletine can potently block the open state of skeletal muscle Na^+ channels because of its efficacy in patients with myotonia. To address this question we expressed wild-type and inactivation-deficient hNav1.4 Na^+ channels (hNav1.4-L443C/A444W) in HEK293t cells and compared their state-dependent block by mexiletine. We selected this mutant human Nav1.4 mutant muscle channel because it expressed well in HEK293t cells and displayed an inactivation-deficient phenotype similar to that in the rat rNav1.4-L437C/A438W muscle Na^+ channel (Wang *et al.* 2003). We found that hNav1.4 Na^+ channels exhibited three distinct affinities for mexiletine, with the open state of the inactivation-deficient mutant channels showing the highest affinity (IC_{50} = 3.3 μM), the inactivated state showing an intermediate affinity (67.8 μM), and the resting state of the wild-type channel showing the weakest affinity (431.2 μM). The presence of a large persistent late Na^+ current in this mutant during prolonged depolarization also allowed us to measure directly the time-dependent block at various mexiletine concentrations. Such measurements yielded an on-rate of 10.4 μM^{-1} s^{-1} and an off-rate of 54.4 s^{-1} for the open-channel block of mexiletine at +30 mV.

Methods

Site-directed mutagenesis

We used the QuikChange XL Site-Directed Mutagenesis Kit (Stratagene, La Jolla, CA, USA) to create a human skeletal muscle hNav1.4-L443C/A448W mutant clone (Wang *et al.* 2003). The hNav1.4 wild-type Na^+ channel clone in the pRc/CMV vector was a generous gift from Dr T. R. Cummins (Yale University). We also created homologous clones of cardiac hNav1.5-L409C/A410W and an additional mutation F1760K in the hNav1.5-L409C/A410W backbone. The F1760 position at D4S6 is known to be critical for binding of antiarrhythmic agents and LAs (Ragsdale *et al.* 1994, 1996; Nau *et al.* 2000). These homologous clones displayed inactivation-deficient phenotypes comparable to those of their rNav1.4 counterparts (Wang *et al.* 2003).

Transient transfection

Human embryonic kidney cells (HEK293t) were grown to ~50% confluence in DMEM (Life Technologies, Inc., Rockville, MD, USA) containing 10% fetal bovine serum (HyClone, Logan, UT, USA), 1% penicillin and streptomycin solution (Sigma, St Louis, MO, USA), 3 mM taurine, and 25 mM Hepes (Life Technologies, Inc.) and then transfected by a calcium phosphate precipitation method (Cannon & Strittmatter, 1993). Transfection of hNav1.4-pRc/CMV or other mutant clones (5–10 μg) along with rat β1-pcDNA1/Amp (10–20 μg) and reporter CD8-pih3m (1 μg) was adequate for current recording. Cells were replated 15 h after transfection in 35 mm dishes, maintained at 37°C in a 5% CO_2 incubator, and used after 1–4 days. Transfection-positive cells were identified with immunobeads (CD8-Dynabeads, Lake Success, NY, USA).

Whole-cell voltage clamp

The whole-cell configuration was used to record Na^+ currents (Hamill *et al.* 1981). Borosilicate micropipettes (Drummond Scientific Company, Broomall, PA, USA) were pulled with a puller (P-87, Sutter Instrument Company, Novato, CA, USA) and heat polished. Pipette electrodes contained 100 mM NaF, 30 mM NaCl, 10 mM EGTA, and 10 mM Hepes, adjusted to pH 7.2 with CsOH. The pipette electrodes had a tip resistance of 0.5–1.0 MΩ. Access resistance was 1–2 MΩ and was further reduced by series resistance compensation. All experiments were performed at room temperature (22–24°C) under a Na^+-containing bath solution with 65 mM NaCl, 85 mM choline chloride, 2 mM $CaCl_2$, and 10 mM Hepes, adjusted to pH 7.4 with tetramethyl-ammonium hydroxide. Mexiletine hydrochloride was purchased from Sigma and dissolved in DMSO solution at 100 mM as stock solution. Final mexiletine concentrations were prepared from stock by serial dilution with bath solution. Chloramine-T was obtained from Fisher Chemicals (Fairlawn, NJ, USA) and freshly prepared at a final concentration of 0.5 mM. Tetrodotoxin (TTX) was purchased from Calbiochem-Navabiochem (San Diego, CA, USA). Whole-cell currents were measured by an Axopatch 200B amplifier (Axon Instruments, Foster City, CA, USA) or an EPC-7 amplifier (List Electronics, Darmstadt/Eberstadt, Germany), filtered at 3 kHz, collected, and analysed with pCLAMP8 software (Axon Instruments). The holding potential was set at –140 mV. Leak and capacitance were subtracted by the patch clamp device and further by the leak subtraction protocol (*P*/–4). Voltage error was <4 mV after series resistance compensation. A Student's unpaired *t* test was used to evaluate estimated parameters (mean ± S.E.M. or fitted value ± S.E.M. of the fit); *P* values of <0.05 were considered statistically significant.

Results

Families of Na^+ currents before and after mexiletine treatment

Superimposed current traces of wild-type hNav1.4 Na^+ channels at various voltages were recorded before and after 100 μM mexiletine application (Fig. 1*A* and *B*, respectively). At this concentration, the peak currents were reduced only slightly (~10%) with minimal effects on current kinetics. The peak currents were measured, converted to Na^+ conductance (g_m), normalized, plotted against the corresponding voltage, and fitted with a Boltzmann equation (Fig. 1*C*). The midpoint voltage ($V_{0.5}$) was shifted leftward by 5.1 mV and the slope became steeper after mexiletine treatment ($P < 0.05$).

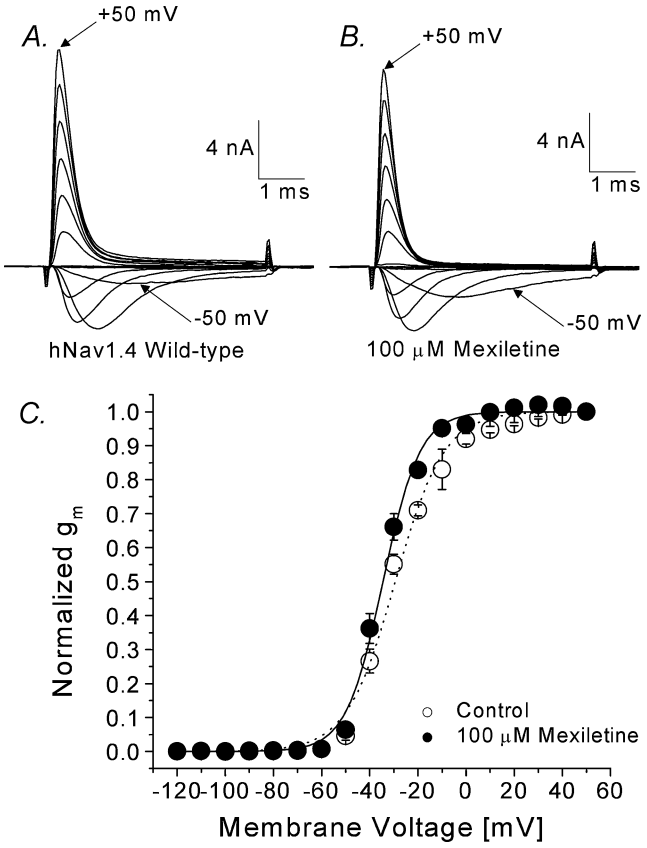

Figure 1. Activation of hNav1.4 wild-type channels in the absence and presence of 100 μm mexiletine
Currents were evoked by 5 ms test pulses from –120 to +50 mV in 10 mV increments without (*A*) or with (*B*) 100 μM mexiletine. The inward current evoked by a pulse to –50 mV and the outward current evoked by a pulse to +50 mV are labelled. *C*, normalized membrane conductance (g_m) was plotted against the corresponding membrane voltage. g_m was determined from the equation $g_m = I_{Na}/(E_m - E_{Na})$, where I_{Na} is the peak current, E_m is the amplitude of the voltage step, and E_{Na} is the estimated reversal potential of the Na^+ current. Plots were fitted with a Boltzmann function, $y = 1/\{1 + \exp[(V_{0.5} - V)/k]\}$. The average midpoint voltage ($V_{0.5}$) and slope (k) for hNav1.4 wild-type (○, $n = 7$; fitted value ± S.E.M. of the fit) were –29.4 ± 0.7 mV and 10.1 ± 0.7 mV, respectively, and –34.5 ± 0.5 mV and 7.6 ± 0.4 mV for the mexiletine-treated cell (●, $n = 5$; $P < 0.05$), respectively. Cells were cotransfected with the β1 subunit. Holding potential was set at –140 mV and the time interval between pulses was 10 s.

Steady-state inactivation before and after mexiletine application

We measured the steady-state inactivation before and after 100 μM mexiletine using a conventional two-pulse protocol. Figure 2*A* and *B* show the superimposed

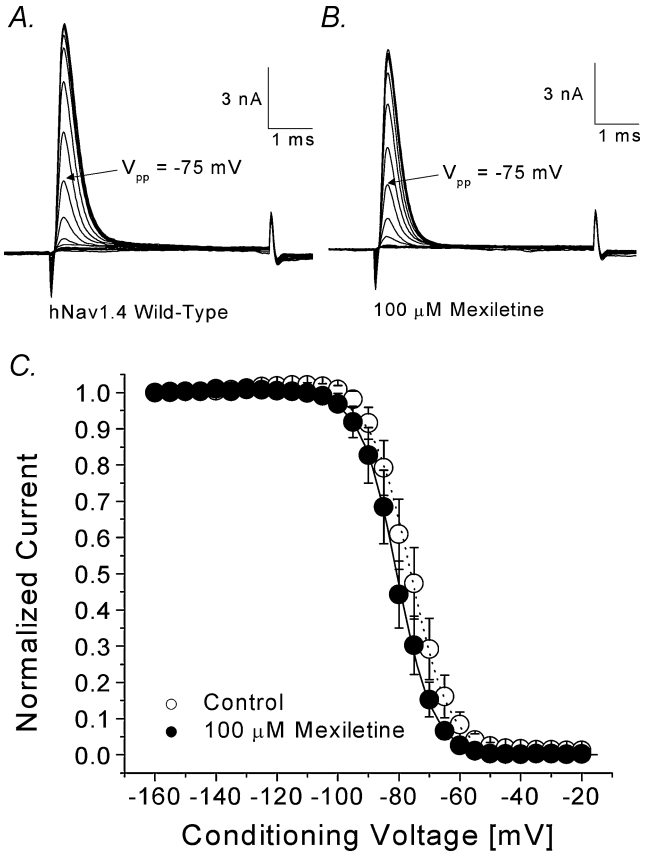

Figure 2. Steady-state inactivation of hNav1.4 with or without 100 μm mexiletine
Currents were evoked by a 5 ms test pulse to +30 mV in the absence (*A*) or presence (*B*) of 100 μM mexiletine. Test pulses were preceded by 100 ms conditioning pulses, increased in 5 mV increments between –160 mV and –120 mV. The interval between pulses was 10 s. *C*, normalized Na^+ current availability (h_∞) of hNav1.4 was obtained from data as shown in *A* and *B* and plotted against the conditioning voltage. Data were fitted with the Boltzmann function, $y = 1/\{1 + \exp[(V - V_{0.5})/k]\}$. The average midpoint ($V_{0.5}$) and slope factor ($k$) for the wild-type (○, $n = 8$) were –75.9 ± 0.2 mV and 6.4 ± 0.2 mV, respectively, and –80.6 ± 0.2 mV and 5.9 ± 0.2 mV for the cells treated with mexiletine (●, $n = 5$). The difference between two $V_{0.5}$ values is significant ($P < 0.05$).

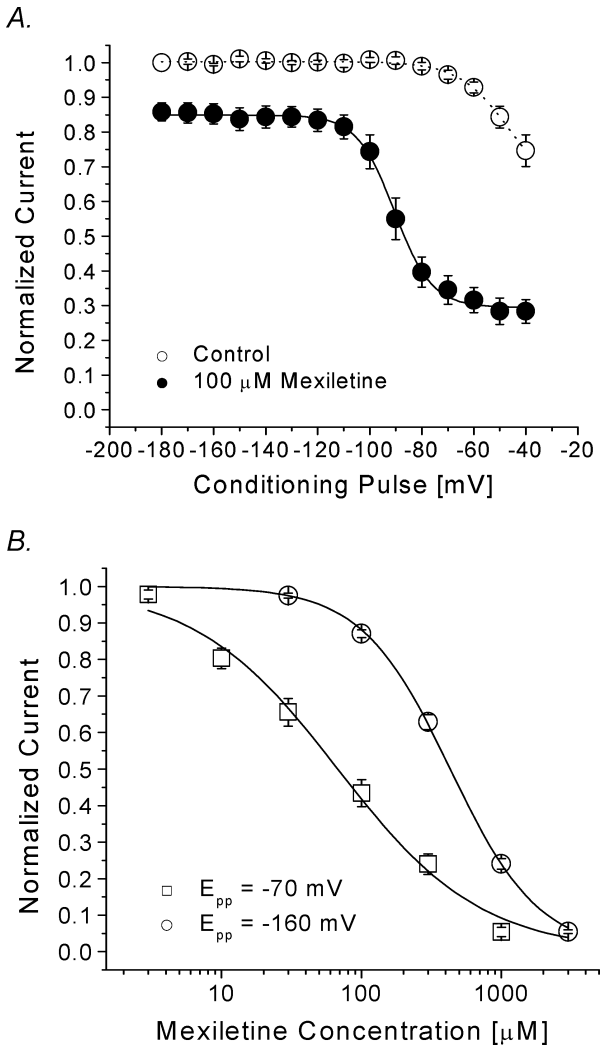

Figure 3. Voltage-dependent block of hNav1.4 by 100 μm mexiletine

A, a 10 s conditioning prepulse ranging in amplitude from –180 to –40 mV was applied. After a 100 ms interval at –140 mV, Na^+ currents were evoked by the delivery of a 5 ms test pulse at +30 mV. Currents obtained in control solution and with 100 μM mexiletine were normalized to the current obtained with the –180 mV control conditioning pulse. Mexiletine data were then renormalized at each conditioning pulse voltage. Normalized control data (○, $n = 6$) and renormalized mexiletine data (●, $n = 5$) were plotted against the conditioning prepulse voltages. Mexiletine data were fitted with a Boltzmann function ($1/[1 + \exp((V_{0.5} - V)/k_E)]$). The average $V_{0.5}$ and k_E (slope factor) values for the fitted functions were –91.8 ± 0.5 mV and 7.2 ± 0.5 mV, respectively. *B*, a 10 s conditioning pulse to –70 mV or –160 mV was followed by a 100 ms interval at –140 mV and a 5 ms test pulse to +30 mV to evoke Na^+ current. Pulses were delivered at 30 s intervals. The peak amplitudes of Na^+ current were measured at various mexiletine concentrations, normalized to the peak amplitude of the control, and plotted against drug concentration. Continuous lines represent fits to the data with the Hill equation. IC_{50} values ± S.E.M. and Hill coefficients ± S.E.M. (in square brackets) for inactivated-state block at –70 mV (□, $n = 5$), and for the resting-state block at –160 mV (○, $n = 5$) are 67.8 ± 7.0 μM [0.85 ± 0.07], and 431.2 ± 9.4 μM [1.3 ± 0.3], respectively.

current traces elicited by a test pulse of +30 mV with various conditioning pulses. Peak currents were measured, normalized with respect to the maximal amplitude at the conditioning voltage of –160 mV, plotted against conditioning voltages, and fitted with a Bolzmann equation (Fig. 2*C*). The midpoint voltage ($V_{0.5}$) was shifted leftward by 4.7 mV ($P < 0.05$) and the slope factor was not significantly changed.

Determination of resting and inactivated affinities

To measure the resting and inactivated affinities for mexiletine, we first determined whether saturable low and high affinities for this drug exist in hNav1.4 Na^+ channels using a voltage-scanning protocol. A 10 s conditioning pulse at various voltages ranging from –180 to –40 mV was applied to allow mexiletine (100 μM) to bind with its receptor. Following a 100 ms interval at –140 mV, a test pulse at +30 mV was used to measure the remaining currents. Peak currents were measured, normalized, and plotted against voltages (Fig. 3*A*). We found that there are two types of mexiletine block: one low-affinity block at voltages from –180 to –120 mV and one higher-affinity block at voltages from –70 to –40 mV. The dose–response curves were subsequently constructed at –160 and –70 mV and fitted with a Hill equation to obtain the resting- and inactivated-state block by mexiletine (Fig. 3*B*). The IC_{50} values were 67.8 ± 7.0 μM [Hill coefficient, 0.85 ± 0.07] at –70 mV for the inactivated-state affinity and 431.2 ± 9.4 μM [1.3 ± 0.1] ($n = 5$) for the resting-state affinity. These values are comparable to the values reported by Takahashi & Cannon (2001) (28.3 μM and 650 μM for the inactivated- and resting-state affinities, respectively) under different ionic conditions and pulse protocols.

Development of and recovery from mexiletine-induced inactivated-state block

The development of inactivated-state block by mexiletine was measured using a pulse protocol shown in Fig. 4*A* (top). We found that the inactivated-state block reached its steady-state condition after a 1 s conditioning pulse at –50 mV with a time constant of 203 ± 11 ms ($n = 5$).

The recovery from the inactivated-state block was measured using the pulse protocols shown in Fig. 4*B* (top). With a 100 ms conditioning pulse at –50 mV, the level of block was ∼30% (Fig. 4*B*, ○), and the time constant of recovery was 0.74 ± 0.06 s ($n = 5$), while 70% of normal Na^+ channels recovered as rapidly from their inactivated state as those found in the control (□). With a 500 ms conditioning pulse at –50 mV, the level of block was

increased to ~60% (Fig. 4*B*, ●), but recovery had the same slow time constant of 0.70 ± 0.03 s ($n = 5$) as that with a 100 ms conditioning pulse.

Families of inactivation-deficient Na^+ currents before and after mexiletine treatment

Superimposed Na^+ current traces of inactivation-deficient hNav1.4-L443C/A444W mutant channels at various voltages were recorded before and after 100 μM mexiletine application (Fig. 5*A* and *B*). The mutant current decayed more slowly and incompletely than the wild-type current (Fig. 5*A* *versus* Fig. 1*A*). A significant amount of Na^+ current was maintained at the end of test pulses. With 100 μM mexiletine, the currents decayed rapidly (Fig. 5*B*) as if the maintained currents were potently blocked by mexiletine. The peak currents were measured, converted to conductance (g_m), normalized, plotted against the membrane voltage, and fitted with a Boltzmann equation (Fig. 5*C*). The midpoint voltage ($V_{0.5}$) was shifted leftward by 17 mV ($P < 0.05$) and the slope factor was smaller (14.8 mV *versus* 17.0 mV; $P < 0.05$). It is unclear why mexiletine elicits these changes in Na^+ channels, but related smaller changes also exist in wild-type channel (Fig. 1*C*).

Steady-state inactivation of hNav1.4-L443C/A444W mutant Na^+ channels before and after mexiletine application

Since residual fast inactivation was evident in current traces, we measured the steady-state fast inactivation using a conventional two-pulse protocol as described in Fig. 2. Figure 6*A* and *B* shows the current traces with conditioning pulses ranging from –160 to –15 mV before and after 100 μM mexiletine application. With mexiletine, the decaying phase of the Na^+ currents was rapid (Fig. 6*B*),

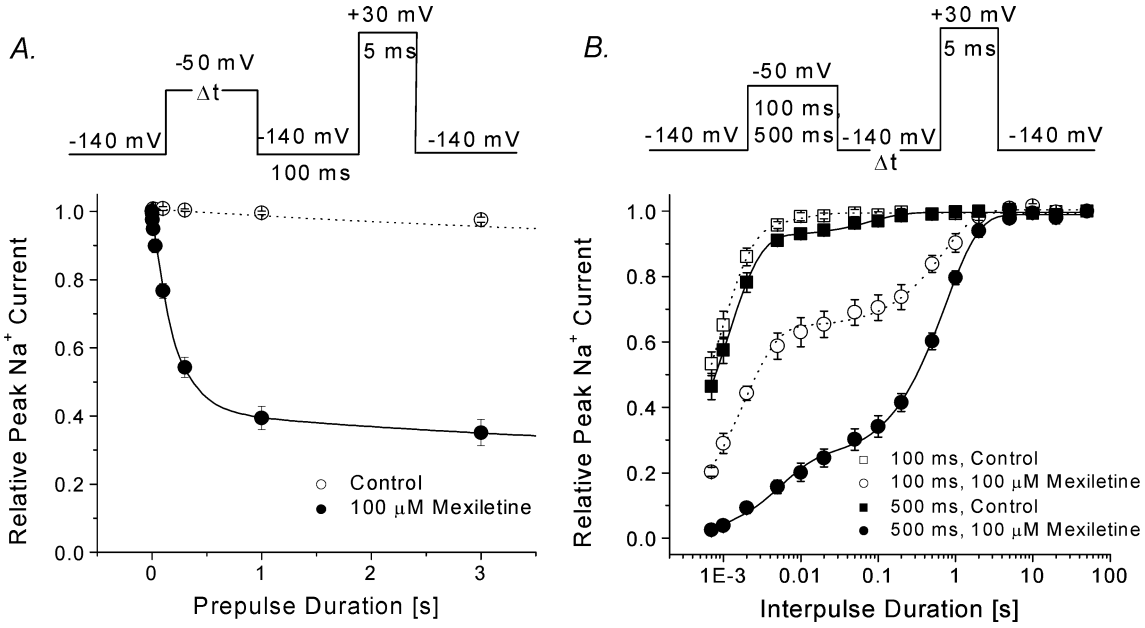

Figure 4. Development of and recovery from the inactivated-state block of hNav1.4 by 100 μm mexiletine

A, for the development of the inactivated block, the pulse protocol shown at the top was applied. The peak currents at the test pulse were measured and normalized to the initial peak amplitude ($t = 0$) and plotted against the prepulse duration. The data were fitted by a single-exponential function or, where appropriate, a double-exponential function. The fast time constant for mexiletine-treated cells (●, $n = 5$) was 0.203 ± 0.011 s. The slow time constant in the control ($\tau = 5.9 \pm 1.3$ s; ○, $n = 7$) and in mexiletine-treated cells ($\tau = 5.7 \pm 1.0$ s; $n = 5$) probably represents the slow inactivation of the Na^+ channel. *B*, the recovery from the inactivated-state block was measured by the pulse protocol shown at the top. The peak currents at the test pulse were measured, normalized and plotted against the interpulse duration. The recovery time courses were fitted by the sum of two exponentials. The fast and slow time constants for the 100 ms conditioning pulse were 0.8 ± 0.1 ms and 8.0 ± 0.3 ms (control, □, $n = 5$), and 2.0 ± 0.2 ms and 0.70 ± 0.06 s (mexiletine, ○, $n = 5$). The fast and slow time constants for the 500 ms conditioning pulse were 1.0 ± 0.1 ms and 0.080 ± 0.015 s (control, ■, $n = 5$), and 5.1 ± 0.7 ms and 0.74 ± 0.03 s (mexiletine, ●, $n = 5$). The slow time constant represented the recovery from the inactivated-state block by mexiletine.

suggesting a rapid time-dependent block of the open Na^+ channels. The peak currents were measured, normalized with respect to the maximal value, plotted against the conditioning voltage, and fitted with a Bolzmann equation. Without mexiletine, about 60% of peak currents were non-inactivating for a 100 ms pulse at –20 mV (Fig. 6*C*; ○). Two Bolzmann equations were used to fit the curve obtained with mexiletine, possibly due to the presence of both inactivated-channel block and open-channel block. Mexiletine blocked more than 95% of peak currents at –20 mV under these conditions (Fig. 6*C*; ●).

If the inactivated channel displayed a higher affinity for mexiletine than the resting channel, we should be able to detect this inactivated-state block using the voltage-scanning protocol described in Fig. 3*A*. Under identical conditions, we were indeed able to detect a higher affinity for the inactivated channel by mexiletine, as shown in Fig. 7, in these inactivation-deficient mutant channels. Based on these results (Figs 6 and 7), we concluded that there are three distinct affinities for mexiletine in hNav1.4 channels. The resting channel exhibited the lowest affinity, the inactivated channel an intermediate affinity, and the open channel the highest affinity. We did not examine the inactivated-state block in inactivation-deficient hNav1.4-L443C/A444W mutant channels in detail since their inactivated state is severely impaired. In any event, the

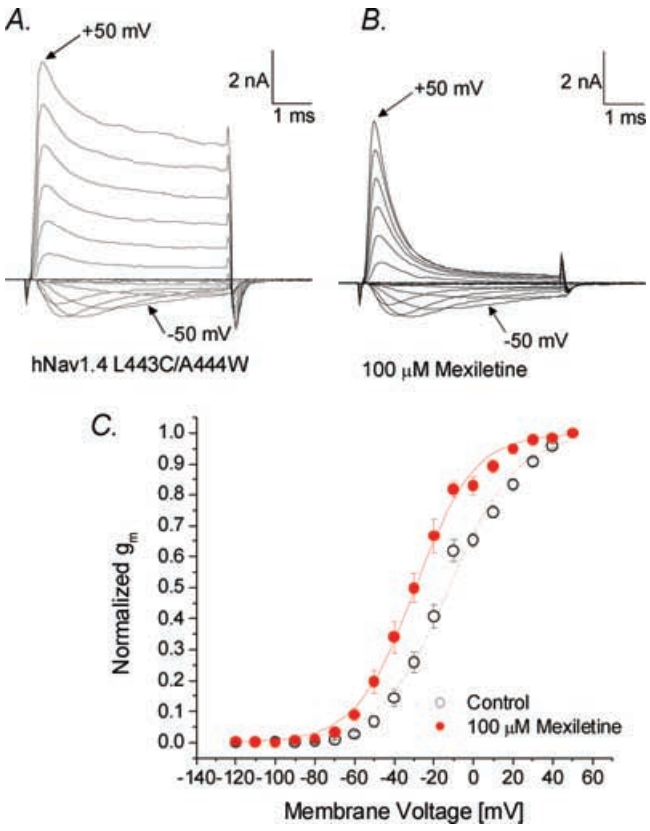

Figure 5. Activation of hNav1.4 l443C/A444W mutant channels without and with mexiletine
Superimposed current traces were evoked by 5 ms pulses from –120 to +50 mV in 10 mV increments in the absence (*A*) or presence (*B*) of 100 μM mexiletine. The inward current evoked by a pulse to –50 mV and the outward current evoked by a pulse to +50 mV are labelled. *C*, normalized membrane conductance (g_m) was plotted against the membrane voltage. g_m was determined as described in Fig. 1*C*. Plots were fitted with a Boltzmann function. The average midpoint voltage ($V_{0.5}$) and the slope factor (k) of the function in the control solution (○, $n = 11$) were –12.4 ± 0.9 mV and 17.0 ± 0.9 mV, respectively, and –29.4 ± 0.7 mV and 14.8 ± 0.6 mV for the mexiletine-treated cell (●, $n = 6$; $P < 0.05$).

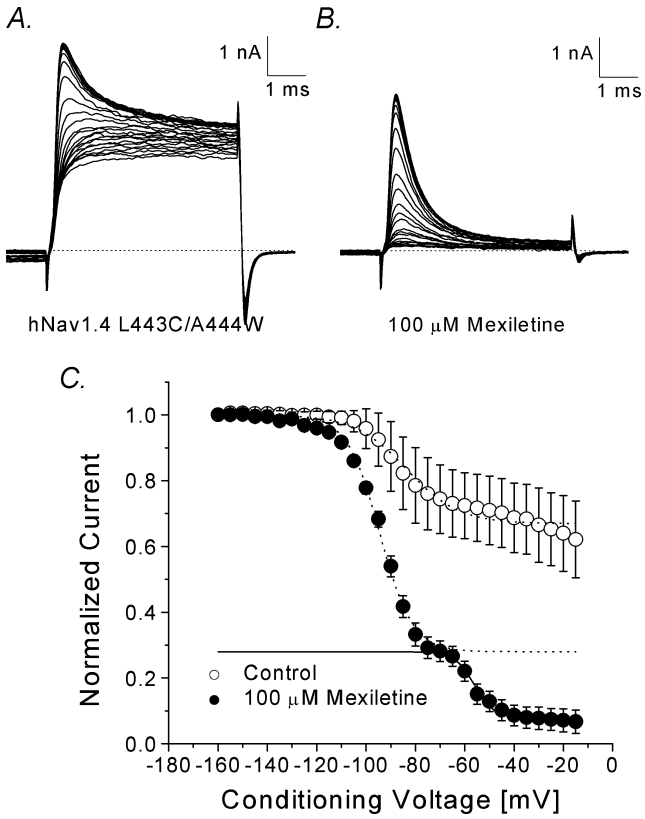

Figure 6. Steady-state inactivation of hNav1.4 l443C/A444W mutant channels without and with mexiletien
Superimposed current traces were evoked by a 5 ms test pulse to +30 mV in the absence (*A*) or presence (*B*) of 100 μM mexiletine. Test pulses were preceded by 100 ms conditioning pulses and increased in 5 mV increments between –160 and –15 mV *C*, peak currents in *A* and *B* were measured and normalized with respect to the amplitude with the –160 mV conditioning pulse and plotted against the conditioning voltage. Plots were fitted with the Boltzmann function as described in Fig. 2*C*. The average midpoint ($V_{0.5}$) and slope factor (k) for the control solution (○, $n = 11$) were –83.6 ± 1.2 mV and 10.6 ± 1.0 mV, respectively, and –88.6 ± 0.7 mV and 11.1 ± 0.6 mV for the cells treated with mexiletine (●, $n = 6$; dashed line). A second Boltzmann function ($V_{0.5} = –57.2 \pm 2.7$ mV; $k = 4.5 \pm 0.2$ mV; continuous line) was applied to fit the mexiletine data.

affinity for mexiletine of the inactivated state in these mutant channels is likely to be similar to that of wild-type based on the similar results obtained using the voltage-scanning protocol (Fig. 3*A* *versus* Fig. 7). A direct measurement of the open-channel affinity is described next.

Open-channel block by mexiletine

To measure directly the open-channel affinity for mexiletine in inactivation-deficient mutant channels, we applied a test pulse of +30 mV with a duration of 50 ms. Figure 8*A* shows current traces before and after mexiletine applications. Without the drug, the inactivation-deficient mutant hNav1.4-L443C/A444W current decayed with biphasic kinetics. The fast decaying phase represented the residual fast inactivation and the slower phase represented the slow inactivation (Wang *et al.* 2003). The persistent late currents were blocked by mexiletine in a dose-dependent manner; higher concentrations elicited a faster time-dependent block and blocked a larger percentage of persistent currents (Fig. 8*A*). This time-dependent block by mexiletine was fitted by an exponential function and the time constant plotted against the concentration (Fig. 8*B*). The on-rate corresponded to the slope of the fitted line and the off-rate corresponded to the *y*-intercept (O'Leary & Chahine, 2002). The on- and off-rates ($n = 5$) of mexiletine block at +30 mV were estimated to be 10.4 ± 1.8 μM^{-1} s^{-1} and 54.4 ± 6.0 s^{-1}, respectively, slightly larger than estimated values for a typical LA, bupivacaine (6–7 μM^{-1} s^{-1} and 20–30 s^{-1}; Valenzuela *et al.* 1995). The calculated equilibrium dissociation constant (K_D = off-rate/on-rate) for mexiletine was 5.2 μM. The dose–response curves for resting-channel and open-channel block were constructed directly from data for peak current block and steady-state block of the persistent currents at the end of the test pulse, respectively (Fig. 8*C*, ○ for the resting block, □ for the open-channel block). The IC_{50} values [Hill coefficients] for resting- and open-channel block were 336.4 ± 20.0 μM [1.2 ± 0.1] and 3.3 ± 0.1 (M [0.92 ± 0.02], respectively ($n = 5$).

To measure the recovery from open-channel block at –140 mV we determined its time course using a pulse protocol similar to that described in Fig. 4*B*. Figure 9 shows that the recovery time course of mexiletine-blocked mutant Na^+ channels is slightly slower than that of the wild-type channels shown in Fig. 4*B*, with a time constant of 0.91 ± 0.0 s (● ($n = 5$) *versus* 0.7 s in Fig. 4*B*; $P < 0.05$). This result indicates that mexiletine binds more rapidly with the open channel and dissociates from its open-channel block slightly more slowly than with the wild-type inactivated channel.

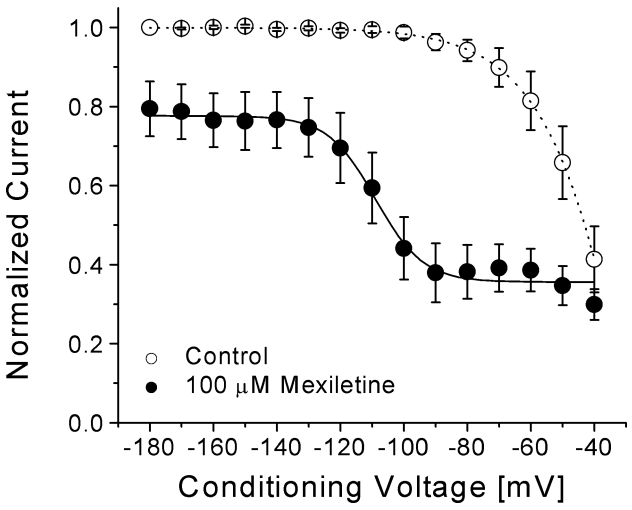

Figure 7. Voltage-dependent block of hNav1.4 l443C/A444W mutant channels by mexiletine
The same pulse protocol as described in Fig. 3*A* was used. Peak currents obtained in control solution and with 100 μM mexiletine were normalized to the peak current obtained at the –180 mV control conditioning pulse. Mexiletine data were then renormalized at each conditioning pulse voltage. Normalized control data (○, $n = 8$) and renormalized mexiletine data (●, $n = 5$) were plotted against the conditioning voltages. Data were fitted with a Boltzmann function ($1/[1 + \exp((V_{0.5} - V)/k)]$). The average $V_{0.5}$ and k (slope factor) values for the fitted functions were –108.9 ± 1.4 mV and 7.5 ± 1.3 mV, respectively, for mexiletine. Notice that the slow inactivation is more pronounced in the inactivation-deficient mutant channels (○) than in wild-type (Fig. 3*A*).

Use-dependent block by mexiletine

Repetitive pulses elicited an additional mexiletine block in wild-type Na^+ channels, which was termed the use-dependent block. We measured this use-dependent block of wild-type and inactivation-deficient mutant currents with a test pulse of +30 mV for 24 ms at a frequency of 5 Hz. Peak currents were measured, normalized with respect to the amplitude of the first pulse, and plotted against the pulse number. Figure 10*A* shows that the use-dependent block reached a steady-state level within a few pulses that was ~70% of wild-type currents, whereas in inactivation-deficient hNav1.4-L443C/A444W mutant channels, the block achieved a steady-state level rapidly, by the second pulse, that was ~55% of currents remaining (Fig. 10*B*). This result demonstrated that the inactivation-deficient Na^+ channels were more susceptible to mexiletine block during repetitive pulses.

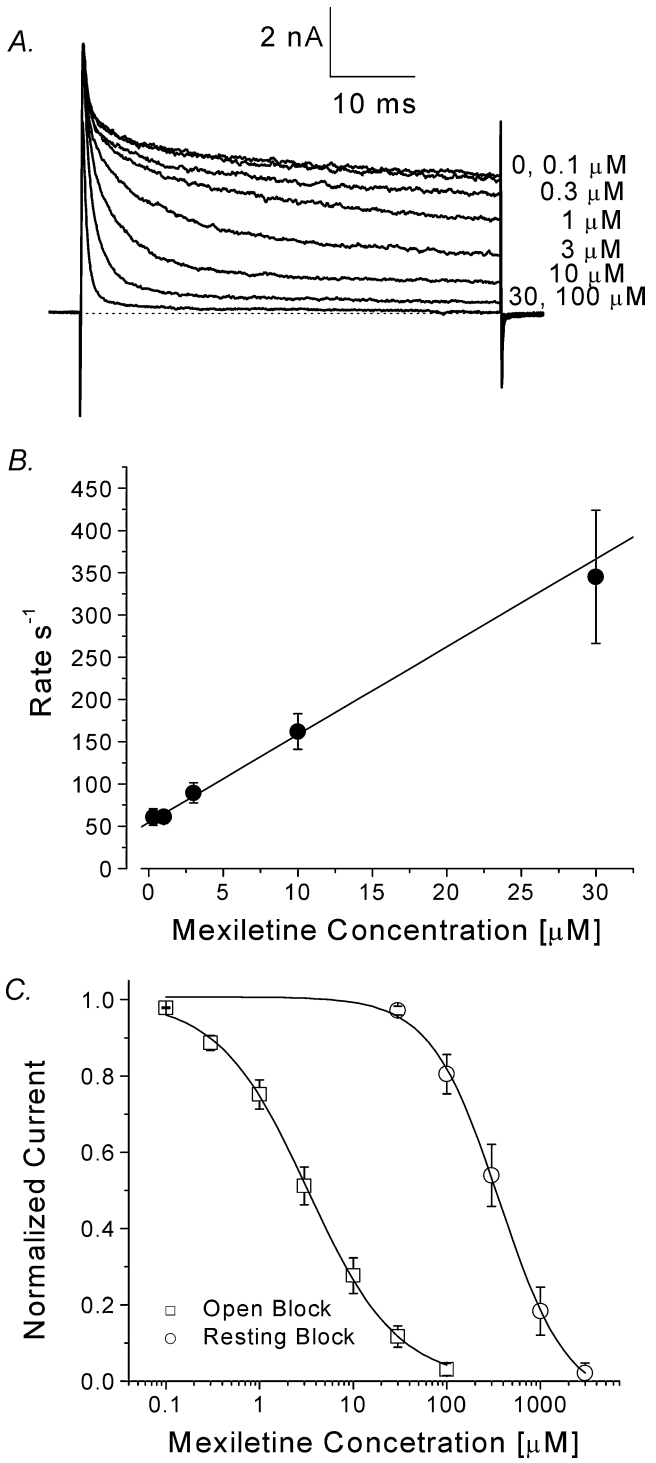

Figure 8. Open-channel block in inactivation-deficient mutant channels by mexiletine

A, superimposed mutant Na^+ currents were recorded at various concentrations of mexiletine. The Na^+ currents were evoked by a 50 ms test pulse to +30 mV every 30 s. A steady state at each concentration was established before application of the next concentrated solution. *B*, the decaying phase of the normalized relative Na^+ current was fitted with a single exponential function, and the corresponding τ value (time constant) was inverted and plotted against the corresponding mexiletine concentration (0.3–30 μM). Data were fitted with a linear regression $y = 10.4x + 54.4$. The on-rate (k_{on}) corresponded to the slope of the fitted line (10.4 μM^{-1} s^{-1}) and the off-rate (k_{off}) corresponded to the *y*-intercept (54.4 s^{-1}). The dissociation constant determined by the equation $K_D = k_{off}/k_{on}$ was 5.2 μM *C*, dose–response curves for open-channel block (relative block at the end of the 50 ms test pulse) and resting-state block (relative block at the peak current) were constructed using the data set as shown in *A*. All pulses were delivered at 30 s intervals. The amplitudes of Na^+ current were measured, normalized to the amplitude of the control, and plotted against the mexiletine concentration. Continuous lines represent fits to the data with the Hill equation. IC_{50} values ± S.E.M. [Hill coefficients ± S.E.M.] are 3.3 ± 0.1 μM [0.90 ± 0.02] for open-channel block (□, $n = 5$), and 336.4 ± 20.0 μM [1.2 ± 0.1] for resting-state block (◯, $n = 5$).

Cardiac inactivation-deficient hNav1.5-L409C/A410W mutant channels and their mexiletine receptor

Since mexiletine is an antiarrhythmic agent targeting human heart Na^+ channels, we measured the potency of open-channel block by mexiletine in human cardiac inactivation-deficient hNav1.5-L409C/A410W mutant Na^+ channels (Fig. 11*A*). Dose–response data show that mexiletine blocked the open-channel with an IC_{50} of 11.1 μM and blocked the resting-channel with an IC_{50} of 157.4 μM (Fig. 11*C*; ■ and □, respectively). The ratio of the resting-channel block *versus* open-channel block was 14.2 in this inactivation-deficient cardiac mutant Na^+ channel. This ratio is less than that found in homologous hNav1.4 mutant channel (or resting/open block = 336 μM/3.3 μM (~100). The reason for this difference is unclear. Previously, Weiser *et al.* (1999) reported that the mexiletine receptor in different isoforms may have different affinities for this drug. We also noticed that the residual fast inactivation in hNav1.5-L409C/A410W mutant channels is minimal, unlike that in hNav1.4-L443C/A444W counterparts (Fig. 11*A versus* Fig. 8*A*).

It has been reported that the Nav1.5-F1760 residue at D4S6 is critical for the binding of traditional LAs (Ragsdale *et al.* 1994; Nau *et al.* 2000). We therefore measured the potency of mexiletine for F1760K in the hNav1.5-L409C/A410W background channel (Fig. 11*B*). The high-affinity block of the F1760K open channel by mexiletine was nearly eliminated, with an IC_{50} of 207.9 μM (Fig. 11; ●), whereas the resting block was less affected, with an IC_{50} of 290 μM (◯). The ratio of resting-channel *versus* open-channel block was only 1.39 in this F1760K inactivation-deficient mutant channel.

Open-channel block by mexiletine in wild-type hNav1.4 Na^+ channels treated with chloramine-T

Chloramine-T is known to impair fast inactivation and generates a significant amount of persistent late Na^+ current (Wang *et al.* 1987). Using this alternative method for fast-inactivation removal, we investigated whether the high-affinity open-channel block by mexiletine also occurs in wild-type hNav1.4 Na^+ channels. Figure 12*A* shows that persistent late Na^+ currents were evident after a brief chloramine-T treatment. These persistent late Na^+ currents were again sensitive to mexiletine in a concentration-dependent manner. The time-dependent block by mexiletine was also apparent but with a slower time course than that shown in inactivation-deficient mutant channels (Fig. 8*A*). Most of these persistent currents originated from hNav1.4 Na^+ channels since they were blocked by 1 μM TTX. Using this type of data set, we constructed the dose–response curve (Fig. 12*B*), which yielded an IC_{50} of 7.5 ± 0.8 μM with a Hill coefficent of 1.0 ± 0.1 ($n = 5$). It is noteworthy that, like site-directed mutagenesis, chemical and/or enzymatic treatment of Na^+ channels may alter the channel structure globally, which in turn may affect the potency of LAs directly or indirectly.

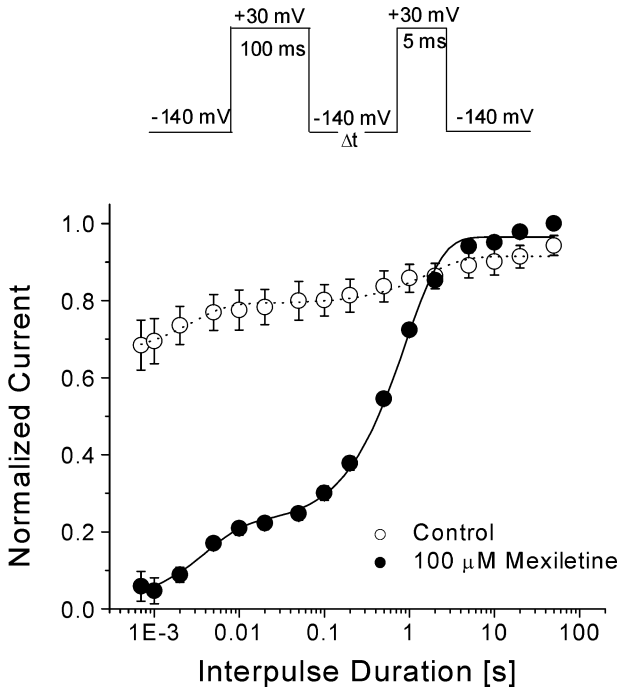

Figure 9. Recovery from the open-channel block of hNav1.4 l443C/A444W mutant channels by 100 μm mexiletine
Recovery time course at –140 mV was measured by the pulse protocol shown at the top and fitted by the sum of two exponentials. The fast and slow time constants for the 100 ms conditioning pulse to +30 mV were 1.7 ± 0.5 s and 3 ± 1 ms (control, ◯, $n = 5$), and 0.91 ± 0.05 s and 4 ± 1 ms (mexiletine, ●, $n = 5$). Notice that most of mutant channels (70%; ◯) are not inactivated by this pulse protocol. However, we might overestimate the slow recovery τ value for mexiletine block since its time course overlapped considerably with that of drug-free mutant channels (~20%; ◯).

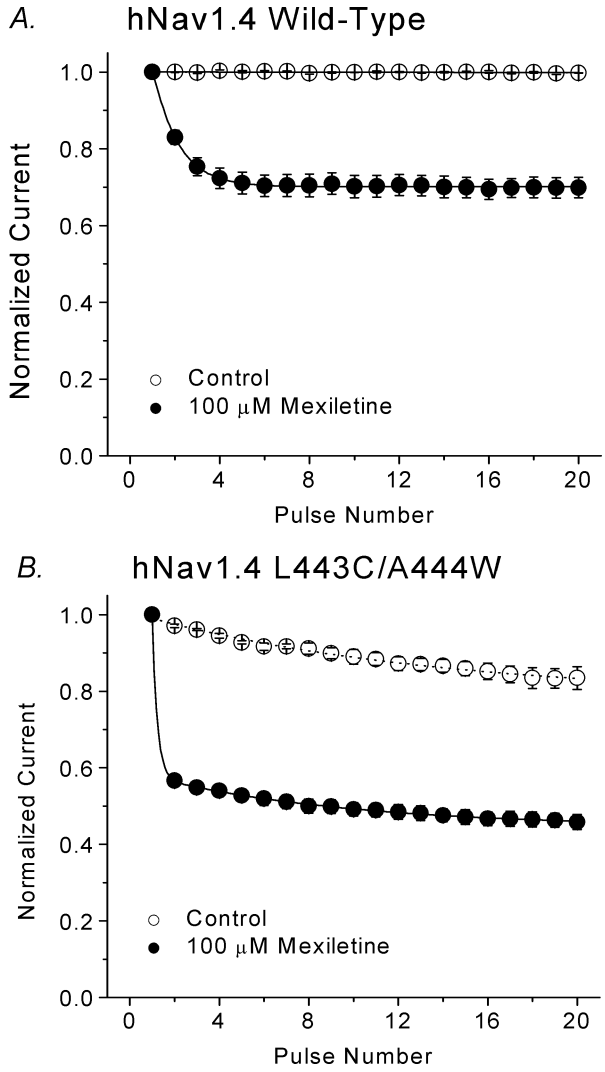

Figure 10. Use-dependent block of hNav1.4 wild-type and inactivation-deficient mutant channels by 100 μm mexiletine
A, twenty 24 ms pulses to +30 mV were delivered to hNav1.4 wild-type channels at 5 Hz from a holding potential of –140 mV. The peak current amplitude of each data set was normalized to the first pulse of the set and plotted against the pulse number. In control solution, the pulse protocol did not elicit use-dependent decreases in current amplitude. Data were best fitted by a single exponential function for 100 μM mexiletine (●, $n = 5$) with a time constant of 1.16 ± 0.03 pulses and reached steady state at 70.1 ± 0.1% of the remaining current (~30% block). *B*, use-dependent block of hNav1.4 l443C/A444W by 100 μM mexiletine was measured as described in *A*. The time constant for the mexiletine solution (●, $n = 7$) was too fast to be measured. Steady state was reached at 48.9 ± 0.6% of the remaining current (~50% block). Most of the persistent currents at the end of 24 ms pulse were blocked by 100 μM mexiletine as shown in Fig. 8*A*.

Previous investigations on the open-channel block of wild-type hNav1.4 Na^+ channels yielded inconsistent results, often dependent on the method of inactivation removal and/or on the type of local anaesthetic used (e.g. Cahalan, 1978; Yeh, 1978; Wang *et al.* 1987).

Discussion

This report demonstrates that mexiletine is a potent open-channel blocker of the human skeletal muscle Na^+ channel, with an IC_{50} of 3.3 μM. Such an open-channel blocking phenotype is also evident in the cardiac Na^+ channel isoform ($IC_{50} = 11.1$ μM). Mexiletine is a class 1b antiarrhythmic agent taken orally. Its therapeutic plasma concentration is in the range 2.8–11 μM for ventricular arrhythmias (Roden, 2001). One of the possible targets for mexiletine *in vivo* is the persistent late Na^+ currents found in normal and failing hearts (Ju *et al.* 1996; Wang *et al.* 1997; Maltsev *et al.* 2001). Mexiletine has also been used to prevent muscle weakness and stiffness in patients with genetic disorders such as paramyotonia congenita (Jackson *et al.* 1994). It is likely that the open-channel block of late Na^+ currents by mexiletine abates the repetitive firing of action potentials that cause myotonic muscle stiffness (Lehmann-Horn & Jurkat-Rott, 1999). We now discuss details of mexiletine actions on hNav1.4 Na^+ channels.

Distinct mexiletine affinities for resting, inactivated and open Na^+ channels

We identified three distinct binding affinities of human skeletal muscle Na^+ channels for mexiletine. The resting-state affinity for mexiletine is weak, with an IC_{50} of 431 μM. The inactivated-state affinity for mexiletine is intermediate, with an IC_{50} of 67.8 μM. In comparison, the open state of hNav1.4 Na^+ channels has the highest affinity for mexiletine, with an IC_{50} of 3.3 μM at +30 mV. This affinity is about 20-fold and 130-fold higher than the inactivated- and resting-state affinities, respectively. The on-rate of the open-channel block by mexiletine was 10.4 μM^{-1} s^{-1} and the off-rate 54 s^{-1} at +30 mV (Fig. 9*B*). The K_D was calculated to be 5.2 μM, which is in fair agreement with the direct IC_{50} measurement.

These kinetic data strongly support the hypothesis that selective targeting of the persistent late Na^+ currents by mexiletine is the basis for its therapeutic intervention, as previously suggested by Wang *et al.* (1997). Their simulations of an ideal antiarrhythmic drug at 10 μM using the on-rate (10 μM^{-1} s^{-1}) and off-rate (30 s^{-1}) for the open-channel block demonstrate that no suppression of peak Na^+ current occurs but marked suppression of the late openings is achieved. Our on- and off-rates for open-channel block by mexiletine (10.4 μM^{-1} s^{-1} and 54 s^{-1}, respectively) are very close to the values of an ideal

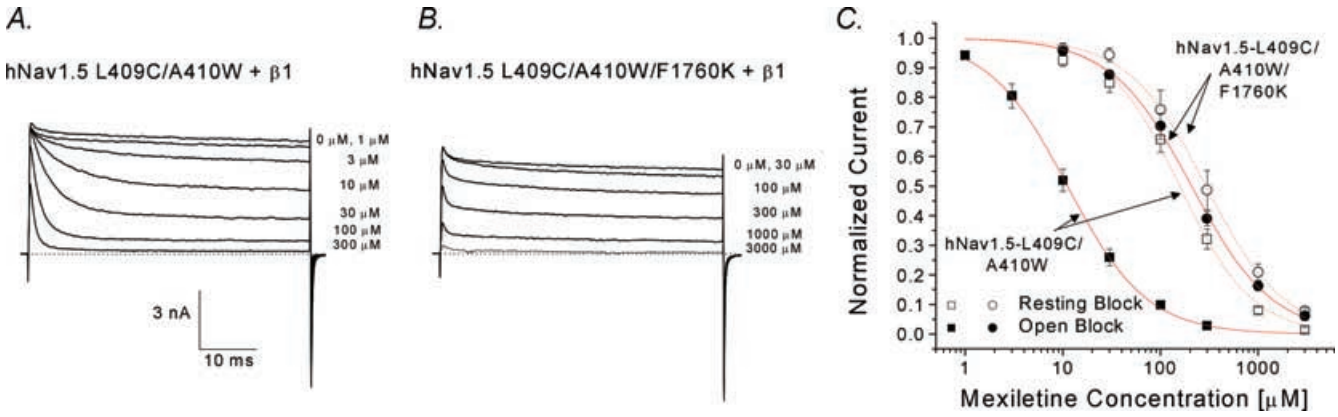

Figure 11. Open-channel block of hNav1.5-L409C/A410W and hNav1.5-L409C/A410W/1760K at various mexiletine concentrations

Superimposed current traces of hNav1.5-L409C/A410W (*A*) or hNav1.5-L409C/A410W/F1760K (*B*) mutant channels were recorded with a test pulse at +30 mV for 50 ms before and after mexiletine at various concentrations. Notice that mutation F1760K renders the open channel relatively resistant to mexiletine block. *C*, dose–response curves for open-channel block (relative block at end of 50 ms test pulse to +30 mV) and resting-state block (relative block of peak currents) were constructed using the data set as shown in *A* and *B*. Data were fitted with the Hill equation. IC_{50} values ± S.E.M. [Hill coefficients ± S.E.M.] for hNav1.5-L409C/A410W are 11.1 ± 0.3 μM [1.1 ± 0.2] for open-channel block (■, $n = 5$), and 157.4 ± 11.4 μM [1.2 ± 0.1] for resting-state block (□, $n = 6$). IC_{50} values ± S.E.M. [Hill coefficients ± S.E.M.] for hNav1.5-L409C/A410W/F1760K are 207.9 ± 7.0 μM [1.0 ± 0.1] for open-state block (●, $n = 5$), and 290.7 ± 9.6 μM [1.1 ± 0.1] for resting-state block (○, $n = 5$).

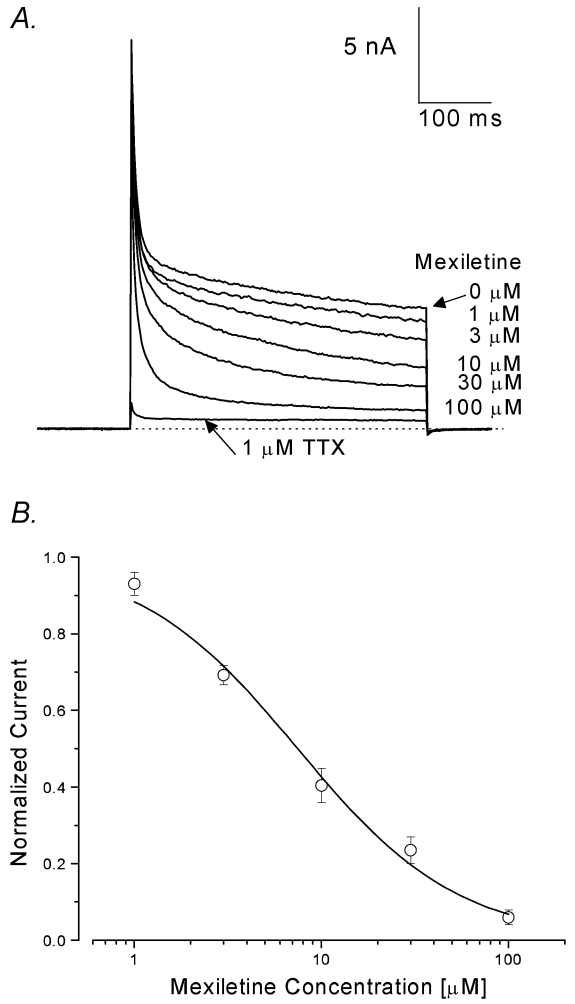

Figure 12. Open-channel block in chloramine-T-treated hNav1.4 Na^+ channels by mexiletine

A, superimposed Na^+ currents were recorded at various concentrations of mexiletine. Before these records were taken, the cell was treated with 0.5 mM chloramine-T for 2.5 min and then washed with drug-free bath solution for 5 min. The Na^+ currents were evoked by a 400 ms test pulse to +30 mV every 30 s. A steady state at each mexiletine concentration was established before application of the next solution. TTX at 1 μM was also applied to identify hNav1.4 Na^+ currents. Treatment with chloramine-T was limited to 2.5 min since prolonged incubation of this oxidant increased the non-linear leak currents. *B*, the dose–response curve for the open-channel block (relative block at the end of the 400 ms test pulse) was constructed using the data set as shown in *A*. All pulses were delivered at 30 s intervals. The amplitudes of Na^+ current were measured, normalized to the amplitude of the control, and plotted against the mexiletine concentration. Leak currents after 1 μM TTX were subtracted from the current measurements. Continuous lines represent fits to the data with the Hill equation. IC_{50} values ± S.E.M [Hill coefficients ± S.E.M.] are 7.5 ± 0.8 μM [1.0 ± 0.1] for open-channel block ($n = 5$). Cells were cotransfected with the β1 subunit.

drug. Simulations with a small off-rate (e.g. 10 s^{-1}) caused suppression of the peak Na^+ currents as well as the late current.

The fact that the open-state block by mexiletine is more effective than the inactivated-state block raises the possibility that mutations at hNav1.4-L443C/A444W residues increase the open-channel affinity preferentially. We think that this is unlikely for three reasons. First, Wang *et al.* (1997) reported that the open-channel block by mexiletine ($IC_{50} = 2$–3 μM) was about 5–10 times higher than the inactivated-state block ($IC_{50} = 15$–20 μM) in all three LQT hNav1.5 Na^+ channels with mutations at three different loci (hNav1.5-(KPQ, N1325S, and R1644H). Unfortunately, it was not possible to measure directly the on-and off-rate kinetics in these mutants because of the small size of persistent currents (5% or less of the peak currents). Second, persistent late Na^+ currents generated by the oxidant chloramine-T also remained sensitive to mexiletine block (Fig. 12), suggesting again that the open channel has a higher affinity for the drug than the resting and the inactivated channels. Third, the high-affinity open-channel block was nearly abolished by a single mutation at D4S6 (Fig. 11*B* and *C*; F1760K in the hNav1.5-L409C/A410W backbone). This phenotype indicates that the LA receptor for mexiletine in this inactivation-deficient mutant channel is comparable to the wild-type and can be further altered by a specific F1760K mutation. Additional investigations on the structure and activity of mexiletine ($pK_a = 9.1$) are needed in order to understand why this specific drug binds preferentially with the open state of the Na^+ channel. The inactivation-deficient muscle hNav1.4-L443C/A444W and cardiac hNav1.5-L409C/A410W mutant Na^+ channels will be suitable for these studies due to their high level of expression in HEK293t cells. These inactivation-deficient mutant channels should also be applicable for the screening of novel open-channel blockers in the future (e.g. De Luca *et al.* 2000).

Use-dependent block and the role of the inactivated block

Use-dependent block of Na^+ currents by antiarrhythmic agents and by LAs arises presumably because these blockers have higher affinities for the open and the inactivated states of the Na^+ channel (Hille, 1977; Hondeghem & Katzung, 1977). In this study we established that the open-channel block by mexiletine played a dominant role in this use-dependent phenomenon (Fig. 10). The development of mexiletine block of the open channel is relatively fast

(Fig. 8*A*). This result suggests that the open-channel block by mexiletine can account for a major portion of the use-dependent block during repetitive pulses found in wild-type or inactivation-deficient mutant Na^+ channels (Fig. 10*A* and *B*).

What then is the role of inactivated-state block by mexiletine *in vivo*? The IC_{50} for inactivated-state block is 67.8 μM, which is 20 times higher than the IC_{50} for the open-channel block (3.3 μM). The development of inactivated-state block by mexiletine at –50 mV has a time constant of 0.203 s for the wild-type hNav1.4 channels. The time constant for the recovery from the inactivated-state block is 0.70 s at –140 mV (Fig. 4*B*). On the basis of these measurements, we concluded that the inactivated block by 100 μM mexiletine has a much slower on-rate than the open block ($\tau < 2$ ms at 100 μM; Fig. 8*A*) and has a slightly faster off-rate than the open-channel block upon repolarization ($\tau = 0.91$ s; Fig. 9). Our dose–response results show that about 20% of inactivated channels are blocked by 10 μM mexiletine (Fig. 3), a concentration that is at the upper end of the therapeutic range (2.8–11 μM). Thus, the inactivated-channel block by mexiletine is also likely to play an important role in modulating the availability of Na^+ channels for action potentials, albeit not as crucial as the open-channel block. Mexiletine at 10 μM will block 75% of late open channels during a 50 ms depolarization. Accordingly, it is likely that mexiletine at a therapeutic concentration will silence persistent late Na^+ channel openings *in vivo* efficiently.

Care should be taken in applying results from heterologous expression studies to the clinical management of patients (Takahashi & Cannon, 2001). Temperature, lipid environment, subunit composition, and additional post-translational modifications of Na^+ channels in myocytes may also affect the degree of inactivated-channel block by mexiletine. Nonetheless, these factors seem unlikely to alter the fact that the open-channel block by mexiletine in human skeletal muscle hNav1.4 Na^+ channels is far more effective than the resting- and inactivated-channel block.

References

Cahalan MD (1978). Local anesthetic block of sodium channels in normal and pronase- treated squid giant axons. *Biophys J* **23**, 285–311.

Cannon SC (2002). An expanding view of the molecular basis of familial periodic paralysis. *Neuromuscular Disorders* **12**, 533–543.

Cannon SC & Strittmatter SM (1993). Functional expression of sodium channel mutations identified in families with periodic paralysis. *Neuron* **10**, 317–326.

Catterall WA & Mackie K (2001). Local anesthetics. In *Goodman and Gilman's the Pharmacological Basis of Therapeutics*, ed.Hardman, JG, Limbird, LE, Molinoff, PB, Ruddon, RW & Gilman, AG, pp. 367–384. Macmillan Publishing Co., New York.

Chabal C, Jacobson L, Mariano A, Chaney E & Britell CW (1992). The use of oral mexiletine for the treatment of pain after peripheral nerve injury. *Anesthesiology* **76**, 513–517.

De Luca A, Natuzzi F, Desaphy JF, Loni G, Lentini G, Franchini C, Tortorella V & Camerino DC (2000). Molecular determinants of mexiletine structure for potent and use-dependent block of skeletal muscle sodium channels. *Mol Pharmacol* **57**, 268–277.

Hamill OP, Marty E, Neher ME, Sakmann B & Sigworth FJ (1981). Improved patch-clamp techniques for high-resolution current recording from cells and cell-free membrane patches. *Pflugers Arch* **391**, 85–100.

Hille B (1977). Local anesthetics: hydrophilic and hydrophobic pathways for the drug receptor reaction. *J General Physiol* **69**, 497–515.

Hille B (2001). Classical mechanisms of block. In *Ion Channels of Excitable Membranes*, pp. 503–536. Sinauer Associate Inc., Sunderland, MA, USA.

Hondeghem LM & Katzung BG (1977). Time- and voltage-dependent interactions of antiarrhythmic drugs with cardiac sodium channels. *Biochim Biophys Acta* **472**, 373–398.

Jackson CE, Barohn RJ & Ptacek LJ (1994). Paramyotonia congenita: abnormal short exercise test, and improvement after mexiletine therapy. *Muscle Nerve* **17**, 763–768.

Ju YK, Saint DA & Gage PW (1996). Hypoxia increases persistent sodium current in rat ventricular myocytes. *J Physiol* **497**, 337–347.

Lehmann-Horn F & Jurkat-Rott K (1999). Voltage-gated ion channels and hereditary disease. *Physiol Rev* **79**, 1317–1372.

Maltsev VA, Sabbah HN & Undrovinas AI (2001). Late sodium current is a novel target for amiodarone: studies in failing human myocardium. *J Mol Cell Cardiol* **33**, 923–932.

Nau C, Wang S-Y, Strichartz GR & Wang GK (2000). Block of human heart hH1 sodium channels by the enantiomers of bupivacaine. *Anesthesiology* **93**, 1022–1033.

O'Leary ME & Chahine M (2002). Cocaine binds to a common site on open and inactivated human heart (Nav1.5) sodium channel. *J Physiol* **541**, 701–716.

Ragsdale DS, McPhee JC, Scheuer T & Catterall WA (1994). Molecular determinants of state-dependent block of Na^+ channels by local anesthetics. *Science* **265**, 1724–1728.

Ragsdale DS, McPhee JC, Scheuer T & Catterall WA (1996). Common molecular determinants of local anesthetic, antiarrhythmic, and anticonvulsant block of voltage-gated Na^+ channels. *Proc Natl Acad Sci U S A* **93**, 9270–9275.

Roden DM (2001). Antiarrhythmic drugs. In *Goodman and Gilman's the Pharmacological Basis of Therapeutics*, ed.Hardman, JG, Limbird, LE, Molinoff, PB, Ruddon, RW & Gilman, AG, pp. 933–970. Macmillan Publishing Co., New York.

Schwartz PJ, Priori SG, Locati EH, Napolitano C, Cantu F, Towbin JA, Keating MT, Hammoude H, Brown AM & Chen LS (1995). Long QT syndrome patients with mutations of the SCN5A and HERG genes have differential responses to Na^+ channel blockade and to increases in heart rate. Implications for gene-specific therapy. *Circulation* **92**, 3381–3386.

Takahashi MP & Cannon SC (2001). Mexiletine block of disease-associated mutations in S6 segments of the human skeletal muscle Na^+ channel. *J Physiol* **537**, 701–714.

Valenzuela C, Snyders DJ, Bennett PB, Tamargo J & Hondeghem LM (1995). Stereoselective block of cardiac sodium channels by bupivacaine in guinea pig ventricular myocytes. *Circulation* **92**, 3014–3024.

Wang DW, Yazawa K, Maita N, George ALJ & Bennett PB (1997). Pharmacological targeting of long QT mutant sodium channels. *J Clin Invest* **99**, 1714–1720.

Wang GK, Brodwick MS, Eaton DC & Strichartz GR (1987). Inhibition of sodium currents by local anesthetics in chloramine-T treated squid axons. *J General Physiol* **89**, 645–667.

Wang S-Y, Bonner K, Russell C & Wang GK (2003). Tryptophan scanning of D1S6 and D4S6 C-termini in voltage-gated sodium channels. *Biophys J* **85**, 911–920.

Weiser T, Qu Y, Catterall WA & Scheuer T (1999). Differential interaction of R-mexiletine with the local anesthetic receptor site on brain and heart sodium channel alpha-subunits. *Mol Pharmacol* **56**, 1238–1244.

Yeh JZ (1978). Sodium inactivation mechanism modulates QA-314 block of sodium channels in squid axons. *Biophys J* **24**, 569–574.

Acknowledgements

This work was supported by grants from NIH (GM48090 and HL66076). We thank Dr T. R. Cummins (Yale University) for providing us with the hNav1.4 clone.